J Mater Sci (2006) 41:8074–8078
DOI 10.1007/s10853-006-0597-3

Crystalline orientation of alumina ceramics prepared by electrophoretic deposition under a high magnetic field

T. Uchikoshi · T. S. Suzuki · Y. Sakka

Received: 18 January 2006 / Accepted: 19 June 2006 / Published online: 2 November 2006

Abstract Electrophoretic deposition (EPD) of alumina in a superconducting magnet was performed at various magnetic field strengths. A stable colloidal suspension of alumina appropriate for magnetic alignment was prepared in an ethanol medium by using a phosphate ester (PE) as a dispersant. The amount of PE appropriate for the stability of the alumina suspension was investigated by measuring the pH, zeta-potential and the relative density of the green compacts. The consolidation of alumina powder was performed by EPD under a magnetic field of 0–12 T. The degree of crystalline orientation of the sintered bodies was evaluated by X-ray diffraction (XRD) as a function of the applied magnetic field during deposition and the sintering temperature.

Introduction

Textured ceramics are currently of much interest for applications in structural and functional ceramics. They have been produced by a variety of techniques; such as tape casting [1, 2], hot forging or deformation [3, 4], and templated or seeded grain growth [5, 6]. Recently, we developed a promising processing technique to fabricate polycrystalline ceramics with preferred crystalline orientation using commercial powder by electrophoretic deposition (EPD) in a strong magnetic field [7–12]. Ceramic particles dispersed in a solvent are rotated due to their magnetic anisotropy and then deposited on a substrate in a DC electric field. A schematic illustration of the concept is shown elsewhere [7].

The fundamental concept is as follows. Many materials in asymmetric (non-cubic) crystalline structures have anisotropic magnetic susceptibilities, $\Delta\chi = \chi_{//} - \chi_{\perp}$, associated with their crystal structures, where $\chi_{//}$ and $\chi_{\perp}$ are the susceptibilities parallel and perpendicular to the magnetic principal axis, respectively. When a single crystal of these materials is placed in a magnetic field, the crystallographic axis of high χ is aligned in the direction of the magnetic field. The driving force of the magnetic alignment is the energy of the crystal anisotropy and is given as

$$\Delta E = \Delta\chi V B^2 / 2\mu_0 \quad (1)$$

where V is the volume of the material, B is the applied magnetic field, and μ_0 is the permeability in a vacuum [13]. The magnetic susceptibilities of feeble magnetic materials ($|\chi| = 10^{-3} \sim 10^{-6}$) are quite low in comparison with those of ferromagnetic materials ($|\chi| = 10^{2} \sim 10^{4}$). Therefore, the ΔE of feeble magnetic materials is much lower than the energy of thermal motion, kT, in a conventional magnetic field generated by a permanent magnet (B = ~10^{-1} T). However, the ΔE can be higher than kT when under a strong magnetic field as high as ~10 T, i.e.,

$$\Delta E > kT \quad (2)$$

and then, even feeble magnetic materials will become orientated.

T. Uchikoshi (✉) · T. S. Suzuki · Y. Sakka
Nano Ceramics Center, National Institute for Materials Science, 1-2-1 Sengen, Tsukuba, Ibaraki 305-004, Japan
e-mail: UCHIKOSHI.Tetsuo@nims.go.jp

Electrophoretic deposition (EPD) processing under a strong magnetic field requires the optimization of the colloidal suspension. For the rotation and orientation of the suspended particles under a magnetic field, each particle must be single crystalline and deflocculated. It is also essential that the colloidal particles in a solvent should be electrostatically stabilized for the electrophoresis. Water is an excellent dispersing medium to prepare stable suspensions with high zeta-potentials, however limited substrate materials must be used to suppress the bubble generation due to the electrolysis of water during the EPD [14].

Phosphate ester (PE) is an effective electrostatic stabilizer which positively charges the particles in organic solvents by donating protons to the powder surface. It has been used as a dispersant in tape casting technology [15, 16]. Recently, it has been reported that the use of PE as a dispersant in nonaqueous solvents offers several advantages for EPD processing [17–21]. However, studies of the effect of PE on EPD processing are still limited.

In this study, we investigated the effect of PE on the characteristics of the suspension stability and EPD in a strong magnetic field.

Experimental procedure

A commercial single-crystalline α-alumina powder (Sumitomo Chem. Co., Ltd., AKP-50, average particle size of 0.2 μm and purity of >99.99%) with the major impurities of Si (13 ppm), Fe (6 ppm), Na (2 ppm), Mg (2 ppm) and Cu (<1 ppm) was used in this study. The magnetic susceptibility χ of the alumina powder, measured with SQUID, was -1.4×10^{-6} emu/cm^3, which indicates the feeble magnetism of the powder. Reagent grade ethanol (>99.5%) was used as the suspension medium. Butoxyethyl acid phosphate $(C_4H_9OC_2H_4O)_nP(O)(OH)_{3-n}$ $n = 1, 2$ (Johoku Chem. Co., Ltd., Japan) was used as an electrostatic stabilizer. Acetic acid and nitric acid were also used to compare the capabilities as dispersing agents with the PE.

10 g of alumina powder per 100 ml of ethanol was dispersed with the PE, and the suspensions of 0–2 wt% PE additions versus the weight of the powder were prepared. The suspensions were ultrasonicated (Model USP-600, Shimadzu, Inc.) at frequency of 20 kHz and power of 160 W for 5 min to break agglomerates, and then were stirred for at least 30 min. A pH meter (Model HM-14P, TOA Electronic, Ltd., Japan) was used to determine the appropriate addition of the PE. The zeta-potential of the alumina suspension was measured by an acoustic and eletroacoustic spectrometer (Model DT-1200, Dispersion Technology, Inc., USA).

It must be noted that the ''operational pH'' measured using a pH meter calibrated for aqueous solvent differs from real pa_H in a nonaqueous solvent; i.e.,

$$\mathrm{pH} - pa_H = \frac{\Delta Ej}{\left(\frac{RT \ln 10}{F}\right)} \tag{3}$$

or

$$\mathrm{pH} - pa_H = \frac{\Delta Ej}{0.05916} \quad (\text{at } 25\,^\circ\,\mathrm{C}) \tag{4}$$

where pa_H (= -loga_H) is the negative logarithm of the proton activity in a nonaqueous solvent, ΔEj is the residual liquid-junction potential encountered in the standardization and testing step of a standard pH meter [22, 23]. For an ethanol suspension, (ΔEj/0.05916) = –1.23 was calculated [24]. In this paper, the operational pH is used for the sake of convenience.

The suspension was placed in a cryogen-free superconducting magnet (JASTEC, Inc., JMTD-12T100NC5). Then a magnetic field of 0–12 T was applied to the suspension to align the c-axis of each alumina particle parallel to the direction of the magnetic field. A schematic illustration of the apparatus is shown elsewhere [9].

The EPD was carried out at a constant voltage condition of 100 V using a DC power supply (Model 2410, Keithley Instruments, Inc., USA). The direction of the electric field was fixed to be parallel to the direction of the magnetic field. Stainless steel or palladium sheets with a working area of 20×20 mm^2 were used as the electrodes. The distance between the cathode and anode was fixed at 20 mm. The samples were dried in air after the deposition and then separated from the substrate. The sintering of the compacts was conducted at 1373–1873 K for 2 h in air without applying a magnetic field. The green and sintered densities of the alumina deposits were measured by Archimedes' method in kerosene. The crystalline orientation of the alumina ceramics was evaluated by X-ray diffraction (XRD).

Results and discussion

Suspension characterization

The operational pH of the suspension as a function of the weight ratio of PE to the powder is shown in Fig. 1. The pH change of the same amount of pure ethanol without powder was also measured for comparison.

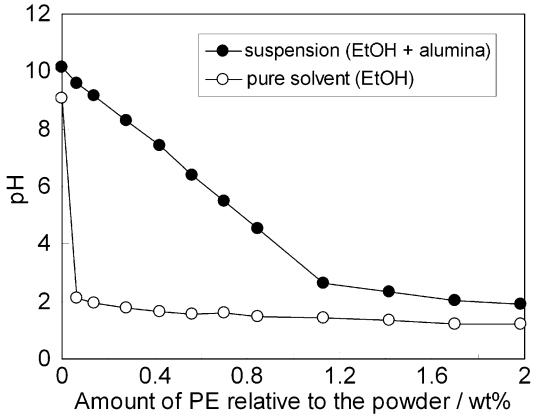

Fig. 1 The operational pH of the suspension as a function of weight ratio of PE to the powder

The PE used in this study was a mixture of mono- and di- PEs. It dissociates in an organic solvent and liberates the protons (or hydronium ions) from the hydroxyl groups bonded to the phosphorus as follows.

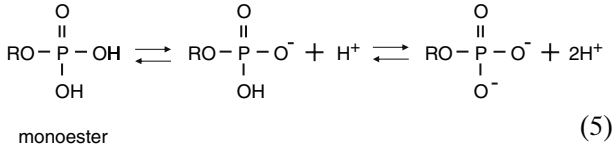

monoester (5)

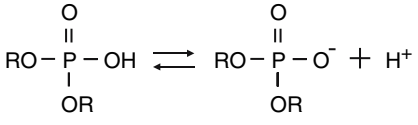

diester (6)

For a pure ethanol solvent, the pH suddenly drops with quite a small amount of PE and then it becomes nearly constant as shown in Fig. 1. This is due to the dissociation of the PE quickly reaching the equilibrium state, and excess PE molecules exist in the neutral state. When a powder exists in the solvent, the liberated protons adsorb on the powder and make the powder surface positively-charged. Therefore, the pH drop of the suspension is delayed as compared with pure solvent. The difference of the two lines reflects the amount of adsorbed protons on the powder. When the amount of PE is increased, the adsorption of protons becomes gradually saturated and the dissociation of PE reaches the equilibrium state. As a result, the dissociation of PE stops and excess PE molecules exist in the neutral state in the suspension. The zeta-potential of the suspension as a function of the amount of PE is shown in Fig. 2. The

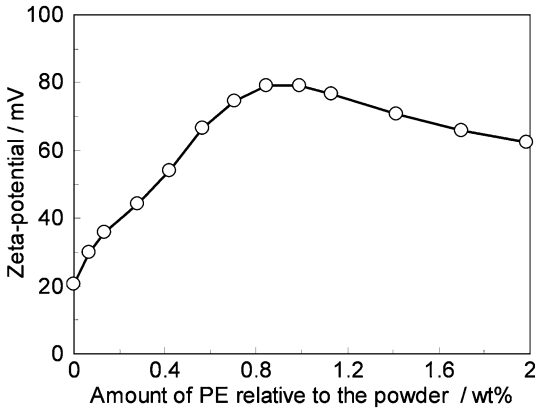

Fig. 2 The zeta-potential of the suspension as a function of the amount of PE

maximum value of the zeta-potential as high as +80 mV is achieved with about 1 wt% of PE addition.

The relative green density of the deposits as a function of the amount of PE is shown in Fig. 3. EPD was conducted without applying a magnetic field to the suspension. The deposits with higher green density are prepared from the suspension with higher zeta-potential. The maximum value of the relative green density was >58%. The relative densities of the green compacts deposited from the alumina/ethanol suspensions prepared with PE, CH_3COOH and HNO_3 are shown in Table 1. To prepare these suspensions, the same alumina powder (AKP-50) and ethanol were used and the pH of all the suspensions was fixed at pH 4.5. The green density of 58.4% from the ethanol + PE suspension is nearly equal to that of the deposits from aqueous suspension [8]. These results show that the combination of ethanol, as a solvent, and PE, as a dispersing agent, is optimal for the preparation of well-dispersed non-aqueous suspensions, promising for

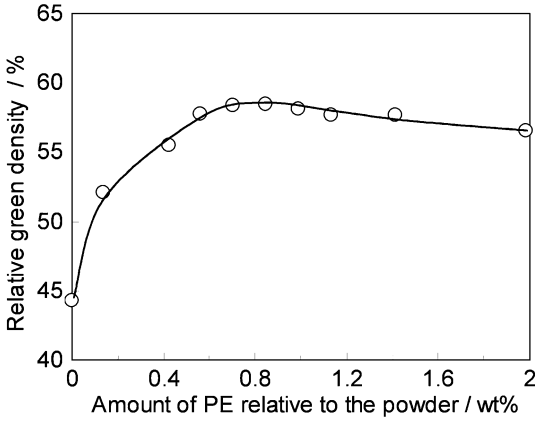

Fig. 3 The relative green density of the deposits as a function of the amount of PE

Table 1 Relative density of the green compacts deposited from the suspensions prepared with different dispersing agents

Solvent + Acid	Green density (%)
Ethanol + Phosphate ester	58.4
Ethanol + Acetic acid	53.5
Ethanol + Nitric acid	53.8

orientation under a strong magnetic field. It is also proposed that the measurement of pH of the suspension is a useful and convenient technique to determine the appropriate addition of PE.

Electrophoretic deposition of the alumina suspension in a magnetic field

The XRD patterns of the alumina deposited at 12 T, followed by sintering at 1873 K is shown in Fig. 4. The difference of diffraction peaks detected to the top and side planes of the compact clearly shows the crystalline orientation. The orientation was not observed in the alumina deposited at 0 T (external to the magnetic field) since it has a randomly oriented polycrystalline structure.

To evaluate the development of the crystalline orientation during sintering numerically, the average orientation angle $\bar{\phi}$ of the crystallites was estimated from the diffraction peaks of the top planes in the 2θ range of 25°–100° using Eq. (7) [24].

$$\bar{\phi} = \frac{\sum (I_{hkl} \times \phi_{hkl})}{\sum I_{hkl}} \tag{7}$$

where ϕ_{hkl} is the interplanar angle between the (*hkl*) planes and the basal plane (*00l*). The ϕ_{hkl} calculated for α-alumina has been listed in our previous report [8].

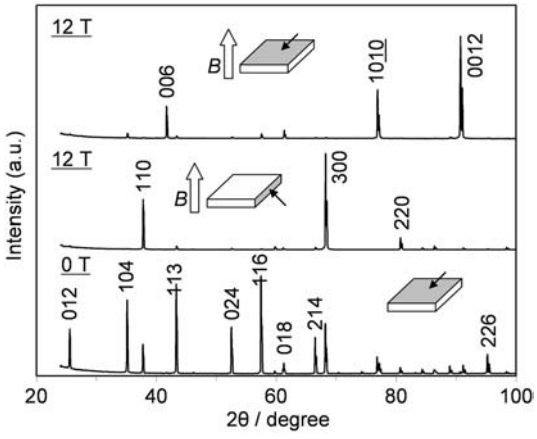

Fig. 4 The XRD patterns of the alumina deposited at 12 T, followed by sintering at 1873 K

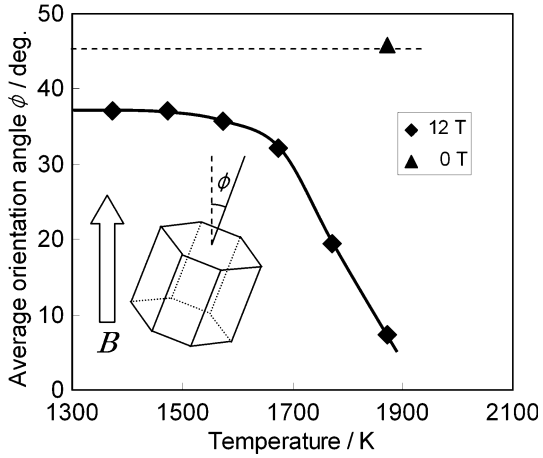

Fig. 5 The average orientation angle $\bar{\phi}$ of the crystallites as a function of sintering temperature

The average orientation angle $\bar{\phi}$ of the crystallites as a function of the sintering temperature is shown in Fig. 5. The crystalline orientation was not so clear at temperatures lower than 1573 K. It is generally known that an improvement in orientation is accompanied by grain growth [8]. A prominent development of the orientation is observed above ~1600 K. The orientation angle $\bar{\phi}$ rapidly decreases with temperature and it reaches 7.3° at 1873 K. The angle $\bar{\phi}$ measured for the samples prepared at 0 T is close to 45°, and it represents a random orientation for the alumina consolidated at 0 T.

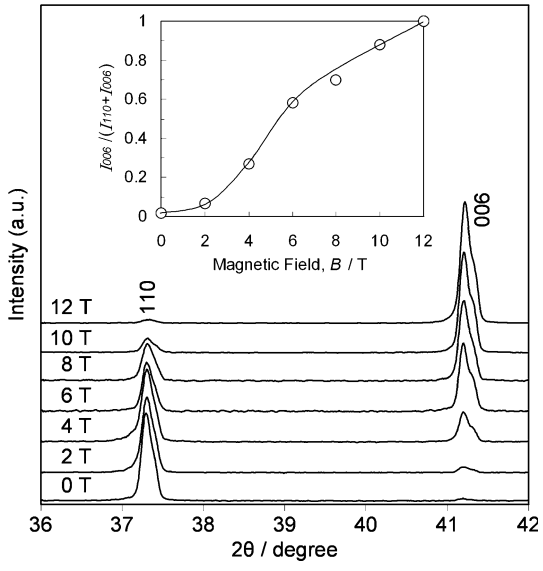

Fig. 6 The changes in the diffraction peaks of the planes (110)(ϕ_{110} = 90°) and (006)(ϕ_{006} = 0°) versus the magnetic field strength

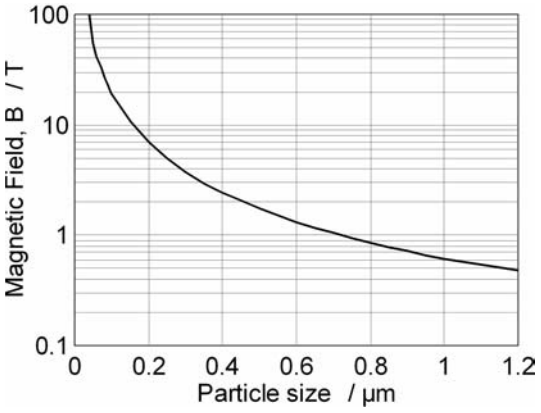

Fig. 7 The critical magnetic field for the orientation of α-alumina at 300 K as a function of particle size

The initial crystalline orientation of green bodies evaluated by XRD showed no obvious differences between the compacts deposited under magnetic fields at 0–12 T. However, the effect of magnetic field strength during the deposition clearly appeared after the sintering at 1873 K. The changes in the diffraction peaks of the planes (110)($\phi_{110} = 90°$) and (006)($\phi_{006} = 0°$) versus the magnetic field strength is shown in Fig. 6. The relative intensity ratios of I_{110} and I_{006} of a randomly-oriented alumina from the JCPDS data #10–173 are 40 and 1, respectively. The change of the intensity ratios $I_{006}/(I_{110} + I_{006})$ is also shown in this figure. The profile of the intensity ratio shows an S-curve: a magnetic field weaker than 2 T is not effective for particle orientation. The orientation obviously increased under magnetic fields of 2–7 T, and highly-oriented structures are obtained under magnetic fields >7 T. The critical magnetic field for the orientation of α-alumina was calculated from eqs. (1) and (2) using the anisotropy of the susceptibility $\Delta\chi = 4.19 \times 10^{-9}$ emu/cm^{-3} [25, 26]. The critical magnetic field for the orientation of α-alumina at 300 K as a function of particle size is show in Fig. 7. The critical magnetic field for a spherical alumina particle of 0.2 μm-size is 6.87 T. The observed orientation of the alumina powder (AKP-50) under magnetic fields weaker than this value is probably due to a broad particle size distribution.

Conclusions

The combination of PE and ethanol provided a good dispersion and surface charging of the alumina particles in an ethanol solvent. A zeta-potential as high as 80 mV was achieved at the saturated amount of the PE adsorption, which was adequate for the orientation of each particle during EPD under a strong magnetic field. A clear crystalline orientation was observed for the compacts deposited under a magnetic field >2 T. Highly-oriented structures were obtained under magnetic fields stronger than 7 T. The average crystalline orientation angle of the alumina deposited under 12 T, followed by sintered at 1873 K, was estimated to be 7.3° from the XRD peaks.

Acknowledgements T. Uchikoshi would like to Dr. S. Novak for her valuable experimental suggestions and Dr. B. D. Hatton for his useful comments. This research was partially supported by the Iketani Science and Technology Foundation and the Grant-in-Aid for Scientific Research from the MEXT.

References

1. Carisey T, Laugierwerth A, Brandon DG (1995) J Eur Ceram Soc 15:1
2. Hall PW, Swinnea JS, Kovar D (2001) J Am Ceram Soc 84:1514
3. Ma Y, Bowman KJ (1991) J Am Ceram Soc 74:2941
4. Yoshizawa Y, Toriyama M, Kanzaki S (2001) J Am Ceam Soc 84:1392
5. Seabaugh MM, Kerscht IH, Messing GL (1997) J Am Ceram Soc 80:1181
6. Suvaci E, Messing GL (2000) J Am Ceram Soc 83:2041
7. Uchikoshi T, Suzuiki TS, Okuyama H, Sakka Y (2003) J Mater Res 18:254
8. Uchikoshi T, Suzuki TS, Okuyama H, Sakka Y (2004) J Mater Sci 39:861
9. Uchikoshi T, Suzuki TS, Okuyama H, Sakka Y (2004) J Mater Res 39:1487
10. Tang F, Uchikoshi T, Suzuki TS, Sakka Y (2004) Mater Res Bull 39:2155
11. Uchikoshi T, Suzuki TS, Iimura S, Tang F, Sakka Y (2006) J Europ Ceram Soc 26:559
12. Suzuki TS, Uchikoshi T., Okuyama H, Sakka Y, Hiraga K (2006) J Eur Ceram Soc 26:661
13. De Rango P, Lees M, Lejay P, Sulpice A, Tournier R, Ingold M, Germi P, Pernet M (1991) Nature 349:770
14. Uchikoshi T, Ozawa K., Hatton BD, Sakka Y (2001) J Mater Res 16:321
15. Chartier T, Streicher E, Boch P (1987) Ceram Bull 66:1653
16. Mikeska T, Cannon WR (1988) Colloids Sur 29:305
17. Zhitomirsky I, Petric A (2000) J Eur Ceram Soc 20:2055
18. Zhitomirsky I (2002) Adv Colloid Interface Sci 97:279
19. Zhitomirsky I, Petric A (2004) J Mater Sci 39:825
20. Uchikoshi T, Furumi S, Suzuki TS, Sakka Y (2006) J Ceram Soc Jpn 114:55
21. Doungdaw S, Uchikoshi T, Noguchi Y, Eamchotchawalit C, Sakka Y (2005) Sci Technol Adv Mater 6:927
22. Sarkar P, Nicholson PS (1996) J Am Ceram Soc 79:1987
23. Wang G, Sarkar P, Nicholson PS (1997) J Am Ceram Soc 80:965
24. Tahashi T, Ishihara M, Sassa K, Asai S (2003) Mater Trans 44:285
25. Uyeda C (1993) Phy Chem Miner 20:77
26. Uyeda C (1993) Jpn J Appl Phys 32:L298